EFFICIENT EXCITATION OF WAVEGUIDES IN CRANK–NICOLSON FDTD

Salvador G. Garcia

Dept. of Electromagnetism, University of Granada
Fuentenueva s/n, 18071 Granada, Spain
e–mail: salva@ugr.es

Fumie Costen

School of Electrical and Electronic Eng. The University of
Manchester
Sackville Street, Manchester M60 1QD, UK
e–mail: fumie.costen@manchester.ac.uk

M. Fernandez Pantoja

Dept. of Electromagnetism, University of Granada
Fuentenueva s/n, 18071 Granada, Spain
e–mail: mario@ugr.es

Luis D. Angulo

Dept. of Electromagnetism, University of Granada
Fuentenueva s/n, 18071 Granada, Spain
e–mail: lmdiazangulo@gmail.com

J. Alvarez

Military Air Sytem, EADS–CASA
Avda. John Lennon s/n. 28906 Getafe, Spain.
e–mail: jesus@ieee.org

Abstract—In this paper we present a procedure to calculate the discrete modes propagated with Crank–Nicolson FDTD in metallic waveguides. This procedure enables the correct excitation of this kind of waveguides at any resolution. The problem is reduced to solving an

eigenvalue equation, which is performed, both in a closed form, for the usual rectangular waveguide, and numerically in the most general case, validated here with a ridged rectangular waveguide.

Key Terms: Crank–Nicolson, FDTD methods, Waveguide excitation, Eigenvalues/eigenfunctions

1. INTRODUCTION

The Finite Difference Time Domain (FDTD) [1] method is one of the most widely used numerical techniques in computational electrodynamics. However, for many problems of interest it may become computationally inefficient, due to the upper limit for the time step imposed by the Courant–Friedrich–Lewy (CFL) stability condition [2]. There is a growing interest in overcoming this limitation by employing unconditionally stable implicit FDTD methods, for which time and space steps can be independently chosen. The unconditionally stable alternating direction implicit (ADI–FDTD) method [3,4] and some of his variations (Locally One Dimensional [5,6], split–step [7], etc.) have received a lot of attraction recently. These approximations suffer up to some extent of numerical errors, which may become severe for some practical applications [8,9].

An alternative to ADI–FDTD based methods, is the Crank–Nicolson FDTD (CN–FDTD) method, for being unconditionally stable beyond the CFL limit, and not presenting the numerical errors found in these [8]. As in the classical FDTD, CN–FDTD replaces the time and space derivatives by second order centered differences, but unlike FDTD, the fields affected by the curl operators are also averaged in time. The resulting scheme is an unconditionally stable fully implicit marching–on–in–time algorithm.

Recently, both iterative preconditioned/non–preconditioned and direct solving of CN–FDTD [10–16] are paving the way to its development, and it is becoming a promising alternative to the classical Yee–FDTD method, which is worth to be extended to include all the features already developed for the classical FDTD method.

Two important problems, which have received a broad attention in literature, arise in the simulation of multimode waveguides by time domain methods: on one hand, the correct excitation of the incident modes at the feeding port and, on the other hand, their subtraction at the end of the guide [17–27].

In this paper, we apply some of these techniques to characterize the discrete modes (also known as mode templates [18]) propagating on arbitrarily–shaped conducting waveguides solved by the Crank–Nicolson Finite Difference Time Domain (CN–FDTD) method. For this purpose we find the solution of the eigenvalue problem numerically, for the general case, and analytically, for rectangular waveguides. The numerical procedure is validated here with a simple ridged rectangular waveguide.

2. DISCRETE PROBLEM

Let us assume a conducting waveguide with arbitrary cross section, filled up with a lossless homogeneous isotropic medium [†] with electrical parameters ε and μ, and consider its axis in the Z direction. The modes propagating in the waveguide must satisfy Maxwell's curl equations, together with the boundary conditions at the metallic walls: null tangential components of the $\vec{E}$ field, and null normal components of the $\vec{H}$ field.

In order to solve this problem with Crank–Nicolson FDTD (CN–FDTD) an average–in–time operator is applied to the fields affected by the space derivatives in Maxwell's curl equations, and all the derivative operators are replaced by the centered difference operator. This results in an unconditionally stable scheme [12], which permits to solve the fields located in the usual Yee–cube spatial disposition with an implicit–in–space marching–on–in–time algorithm

$$\mathcal{D}_u f(u,\dots) = \frac{f(u+\frac{\Delta u}{2},\dots) - f(u-\frac{\Delta u}{2},\dots)}{\Delta u} \qquad (1)$$

$$\mathcal{P}_t f(t,\dots) = \frac{f(t+\frac{\Delta t}{2},\dots) + f(t-\frac{\Delta t}{2},\dots)}{2} \qquad (2)$$

Placing the field components distributed in the usual Yee's cube [1], and using the usual FDTD notation ($\psi^n(i,j,k) \simeq \psi(i\Delta x, j\Delta y, k\Delta z, n\Delta t)$) we can write CN–FDTD as

$$\varepsilon \mathcal{D}_t E_x^{n+\frac{1}{2}}{\scriptstyle(i+\frac{1}{2},j,k)} = \mathcal{P}_t \left(\mathcal{D}_y H_z^{n+\frac{1}{2}}{\scriptstyle(i+\frac{1}{2},j,k)} - \mathcal{D}_z H_y^{n+\frac{1}{2}}{\scriptstyle(i+\frac{1}{2},j,k)} \right) \quad (3)$$

$$\varepsilon \mathcal{D}_t E_y^{n+\frac{1}{2}}{\scriptstyle(i,j+\frac{1}{2},k)} = \mathcal{P}_t \left(\mathcal{D}_z H_x^{n+\frac{1}{2}}{\scriptstyle(i,j+\frac{1}{2},k)} - \mathcal{D}_x H_z^{n+\frac{1}{2}}{\scriptstyle(i,j+\frac{1}{2},k)} \right)$$

$$\varepsilon \mathcal{D}_t E_z^{n+\frac{1}{2}}{\scriptstyle(i,j,k+\frac{1}{2})} = \mathcal{P}_t \left(\mathcal{D}_x H_y^{n+\frac{1}{2}}{\scriptstyle(i,j,k+\frac{1}{2})} - \mathcal{D}_y H_x^{n+\frac{1}{2}}{\scriptstyle(i,j,k+\frac{1}{2})} \right)$$

$$\mu \mathcal{D}_t H_x^{n+\frac{1}{2}}{\scriptstyle(i,j+\frac{1}{2},k+\frac{1}{2})} = \mathcal{P}_t \left(\mathcal{D}_z E_y^{n+\frac{1}{2}}{\scriptstyle(i,j+\frac{1}{2},k+\frac{1}{2})} - \mathcal{D}_y E_z^{n+\frac{1}{2}}{\scriptstyle(i,j+\frac{1}{2},k+\frac{1}{2})} \right)$$

$$\mu \mathcal{D}_t H_y^{n+\frac{1}{2}}{\scriptstyle(i+\frac{1}{2},j,k+\frac{1}{2})} = \mathcal{P}_t \left(\mathcal{D}_x E_z^{n+\frac{1}{2}}{\scriptstyle(i+\frac{1}{2},j,k+\frac{1}{2})} - \mathcal{D}_z E_x^{n+\frac{1}{2}}{\scriptstyle(i+\frac{1}{2},j,k+\frac{1}{2})} \right)$$

$$\mu \mathcal{D}_t H_z^{n+\frac{1}{2}}{\scriptstyle(i+\frac{1}{2},j+\frac{1}{2},k)} = \mathcal{P}_t \left(\mathcal{D}_y E_x^{n+\frac{1}{2}}{\scriptstyle(i+\frac{1}{2},j+\frac{1}{2},k)} - \mathcal{D}_x E_y^{n+\frac{1}{2}}{\scriptstyle(i+\frac{1}{2},j+\frac{1}{2},k)} \right)$$

[†] Although the procedure is shown for simplicity for lossless media, it can be easily formulated for lossy media.

Following the way employed in the non–discrete case, we will search for discrete solutions of (3) with the general form $\Psi^{m_t}(m_x, m_y, m_z) = \Psi_o(m_x, m_y) \, e^{-j\beta_g m_z \Delta z} e^{j\omega m_t \Delta t}$, with β_g being the propagation constant along the waveguide, (m_x, m_y, m_z) integer/semi-integer multiples of the space step, m_t integer/semi-integer multiple of the time-step, and $\Psi_o(m_x, m_y)$ the transversal profile amplitude. For these functions, $\mathcal{D}_z$, $\mathcal{D}_t$ and $\mathcal{P}_t$ have the following eigenvalues respectively

$$a_z = -2j\frac{\sin(\beta_g \frac{\Delta z}{2})}{\Delta z} \;\; , \;\; a_t = 2j\frac{\sin(\omega \frac{\Delta t}{2})}{\Delta t} \;\; , \;\; n_t = \cos(\omega\frac{\Delta t}{2}) \quad (4)$$

The general solution of equations (3), as in the non–discrete case, can be divided into two basic mode sets: Transverse Magnetic (TM), for which $H_z = 0$, and Transverse Electric (TE), for which $E_z = 0$. It can be seen that for both TM and TE modes, it is sufficient to obtain respectively E_{oz} and H_{oz}, to calculate the remaining components. For instance, for the TM polarization (3) is equivalent to

$$E_{ox(i+\frac{1}{2},j)} = \frac{1}{\kappa^2} \left(a_z \mathcal{D}_x E_{oz(i+\frac{1}{2},j)}\right) \tag{5a}$$

$$E_{oy(i,j+\frac{1}{2})} = \frac{1}{\kappa^2} \left(a_z \mathcal{D}_y E_{oz(i,j+\frac{1}{2})}\right) \tag{5b}$$

$$H_{ox(i,j+\frac{1}{2})} = \frac{1}{\kappa^2} \left(\nu_t \varepsilon \mathcal{D}_y E_{oz(i,j+\frac{1}{2})}\right) \tag{5c}$$

$$H_{oy(i+\frac{1}{2},j)} = \frac{-1}{\kappa^2} \left(\nu_t \varepsilon \mathcal{D}_x E_{oz(i+\frac{1}{2},j)}\right) \tag{5d}$$

$$\left(\mathcal{D}_x \mathcal{D}_x + \mathcal{D}_y \mathcal{D}_y + \kappa^2\right) E_{oz(i,j)} = 0 \tag{5e}$$

with the dispersion relationship

$$\kappa^2 = a_z^2 - \mu\varepsilon\nu_t^2 \;\; , \;\; \nu_t = \frac{a_t}{n_t} = 2j\frac{\tan(\omega\frac{\Delta t}{2})}{\Delta t} \tag{6}$$

If we place the staircased conducting walls along the planes of Yee's cube containing the E_z component (Fig. 1), the boundary conditions at the planes parallel to XZ are

$$(a) \, E_{oz(i,j_0)} = 0 \, , \; (b) \, E_{ox(i+\frac{1}{2},j_0)} = 0 \, , \; (c) \, H_{oy(i+\frac{1}{2},j_0)} = 0 \tag{7}$$

and for the planes parallel to YZ

$$(a) \, E_{oz(i_0,j)} = 0 \, , \; (b) \, E_{oy(i_0,j+\frac{1}{2})} = 0 \, , \; (c) \, H_{ox(i_0,j+\frac{1}{2})} = 0 \tag{8}$$

It can easily be deduced from Eqs. (5), that (7a) and (8a) are enough to satisfy the remaining boundary conditions (7b-c) and (8b-c) automatically.
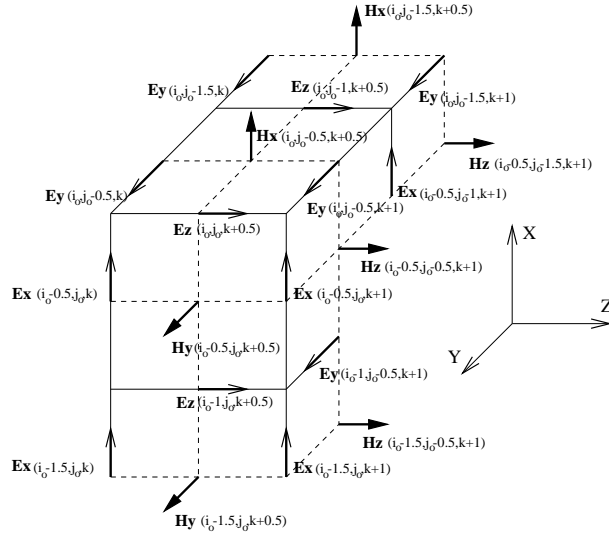
Figure 1. Arrangement of the fields at an edge of the guide

Analogously, the eigenvalue equation for the TE polarization is

$$\left(\mathcal{D}_x\mathcal{D}_x + \mathcal{D}_y\mathcal{D}_y + \kappa^2\right) H_{oz(i+\frac{1}{2},j+\frac{1}{2})} = 0 \qquad (9)$$

Placing the waveguide walls in the same manner as in the TM case, the boundary conditions reduce to

$$\mathcal{D}_y H_{oz(i+\frac{1}{2},j_0)} = 0 \text{ (XZ)}, \quad \mathcal{D}_x H_{oz(i_0,j+\frac{1}{2})} = 0 \text{ (YZ)} \qquad (10)$$

These eigenvalue problems can be solved by numerical techniques, although an analytical solution can be sought in some simple cases. For instance, for a rectangular waveguide, a closed–form solution is shown in Table I. It should be noticed that the non–discrete solution is obtained from the discrete one by replacing the space discrete variables in Table I by the continuous ones, and b_t by ω, b_x by $\frac{p\pi}{a}$, b_y by $\frac{q\pi}{b}$, and b_z by β_g, which are their respective limits when all the increments tend to 0. The FDTD solution is totally similar just replacing $\tan(\omega\frac{\Delta t}{2})$ by $\sin(\omega\frac{\Delta t}{2})$ wherever it appears.

To obtain a discrete numerical solution, for instance in the TE case, we first arrange the values of $H_{oz(i+\frac{1}{2},j+\frac{1}{2})}$ for all the discretized points on the waveguide cross section on a single column vector $\vec{\Phi}$, and then, replacing the transverse discrete Laplacian operator $\mathcal{D}_x\mathcal{D}_x + \mathcal{D}_y\mathcal{D}_y$ by (1), equations (9) and (10) can be explicitly written in matrix form as $\tilde{M}\vec{\Phi} = -\kappa^2\vec{\Phi}$. Since $\tilde{M}$ turns out to be a sparse matrix

Table 1. Closed form of the discrete TE and TM modes for a rectangular waveguide of size $a \times b$

TM (p, q non–null integers, E_o arbitrary)
$E_{ox}\left(i+\frac{1}{2},j\right) = -j\frac{1}{\kappa^2}b_z b_x E_o \cos\left(\frac{p\pi}{a}\left(i+\frac{1}{2}\right)\Delta x\right)\sin\left(\frac{q\pi}{b}j\Delta y\right)$
$E_{oy}\left(i,j+\frac{1}{2}\right) = -j\frac{1}{\kappa^2}b_z b_y E_o \sin\left(\frac{p\pi}{a}i\Delta x\right)\cos\left(\frac{q\pi}{b}\left(j+\frac{1}{2}\right)\Delta y\right)$
$E_{oz(i,j)} = E_o \sin\left(\frac{p\pi}{a}i\Delta x\right)\sin\left(\frac{q\pi}{b}j\Delta y\right)$
$H_{ox}\left(i,j+\frac{1}{2}\right) = j\frac{\varepsilon}{\kappa^2}b_t b_y E_o \sin\left(\frac{p\pi}{a}i\Delta x\right)\cos\left(\frac{q\pi}{b}\left(j+\frac{1}{2}\right)\Delta y\right)$
$H_{oy}\left(i+\frac{1}{2},j\right) = -j\frac{\varepsilon}{\kappa^2}b_t b_x E_o \cos\left(\frac{p\pi}{a}\left(i+\frac{1}{2}\right)\Delta x\right)\sin\left(\frac{q\pi}{b}j\Delta y\right)$
$H_{oz}\left(i+\frac{1}{2},j+\frac{1}{2}\right) = 0$
TE (p, q non simultaneous null integers, H_o arbitrary)
$E_{ox}\left(i+\frac{1}{2},j\right) = j\frac{\mu}{\kappa^2}b_t b_y H_o \cos\left(\frac{p\pi}{a}\left(i+\frac{1}{2}\right)\Delta x\right)\sin\left(\frac{q\pi}{b}j\Delta y\right)$
$E_{oy}\left(i,j+\frac{1}{2}\right) = -j\frac{\mu}{\kappa^2}b_t b_x H_o \sin\left(\frac{p\pi}{a}i\Delta x\right)\cos\left(\frac{q\pi}{b}\left(j+\frac{1}{2}\right)\Delta y\right)$
$E_{oz(i,j)} = 0$
$H_{ox}\left(i,j+\frac{1}{2}\right) = j\frac{1}{\kappa^2}b_z b_x H_o \sin\left(\frac{p\pi}{a}i\Delta x\right)\cos\left(\frac{q\pi}{b}\left(j+\frac{1}{2}\right)\Delta y\right)$
$H_{oy}\left(i+\frac{1}{2},j\right) = j\frac{1}{\kappa^2}b_z b_y H_o \cos\left(\frac{p\pi}{a}\left(i+\frac{1}{2}\right)\Delta x\right)\sin\left(\frac{q\pi}{b}j\Delta y\right)$
$H_{oz}\left(i+\frac{1}{2},j+\frac{1}{2}\right) = H_o \cos\left(\frac{p\pi}{a}\left(i+\frac{1}{2}\right)\Delta x\right)\cos\left(\frac{q\pi}{b}\left(j+\frac{1}{2}\right)\Delta y\right)$
$b_x = \frac{2\sin\left(\frac{p\pi}{a}\frac{\Delta x}{2}\right)}{\Delta x}$, $b_y = \frac{2\sin\left(\frac{q\pi}{b}\frac{\Delta y}{2}\right)}{\Delta y}$, $b_z = \frac{2\sin\left(\beta_g \frac{\Delta z}{2}\right)}{\Delta z}$
$b_t = \frac{2\tan\left(\omega\frac{\Delta t}{2}\right)}{\Delta t}$
$\kappa^2 = 4\frac{\sin^2\left(\frac{p\pi}{a}\frac{\Delta x}{2}\right)}{\Delta x^2} + 4\frac{\sin^2\left(\frac{q\pi}{b}\frac{\Delta y}{2}\right)}{\Delta y^2} = a_z^2 - \nu_t^2\mu\varepsilon$
$\omega_{\text{cutoff}} = \frac{2}{\Delta t}\arcsin\left(\sqrt{\frac{\sin^2\left(\frac{p\pi}{a}\frac{\Delta x}{2}\right)}{(\Delta x/c\Delta t)^2} + \frac{\sin^2\left(\frac{q\pi}{b}\frac{\Delta y}{2}\right)}{(\Delta y/c\Delta t)^2}}\right)$

(no more than 5 non–null elements per line), this eigenvalue problem can be solved using well known linear algebra numerical techniques.

3. IMPLEMENTATION INTO CN–FDTD

The procedure described in [14] has been followed for the implementation of the CN–FDTD equations (3). An iterative Krylov–based solution, employing the BiCGStab solver has been applied. The discrete mode has been fed into the computational space with a total–field/scattered–field formulation implemented by means of an equivalent set of surface currents on two Huygens' planes [2]: one to inject the propagating mode at a plane near one end of waveguide, and the other one close to the other end to suppress it. Simple Mur first order boundary conditions are placed at every end of the waveguide.

4. RESULTS

Using the IMSL eigenvalue routines, we have obtained the TE numerical discrete modes supported by an air–filled ridged rectangular waveguide (Fig. 2(middle)): a total number of 937 modes can propagate in the waveguide [‡]. In order to test the accuracy of the method, we have excited at 3.30 GHz the 9th TE mode, employing for the simulation $\Delta x = \Delta y = 333.3$mm, $\Delta z = 9.0$ mm, $\Delta t = 29.70$ ps. This mode, which has a numerical cutoff frequency of 33.30 MHz, propagates along the Z axis with a low resolution ($\sim$10 cells/wavelength), and it is poorly sampled in time ($\sim$10 samples/period). Fig. 2 shows the H_{oz} pattern of this mode, together with the propagation of E_x along Z at $y = 38\Delta y$, after 1200 time steps. The null field region beginning at $z = 600\Delta z$ (the mode is excited at $z = 400\Delta z$) corresponds to the scattered field zone. Less than 0.01% of the energy escapes from the total field region, which proves the accuracy of the predicted mode propagation. It bears noting that the numerical modes (eigenvectors) found for FDTD are the same as those of CN–FDTD since the space operators of both methods coincide. However the cut–off frequencies (eigenvalues) differ (sinus functions in FDTD and tangent functions in CN–FDTD), and the numerical dispersion also differs. Similar relative deviations between FDTD and CN–FDTD to the ones commented in the next example for the square waveguide are found (see [9] for more details on the dispersion topic).

We have also excited a 10 mm side air–filled square waveguide, with a discrete TM_{11} mode from Table I at 31 GHz. A coarse space–time sampling has been taken $\Delta x = \Delta y = 1.667$ mm, $\Delta z = 1.581$ mm, $\Delta t = 3.12$ ps, which results in $\sim$8 cells/wavelength in the propagation direction, and $\sim$10 samples/period. The CN–FDTD cut–off frequency of this mode is $f_c = 20.67$GHz [§] . Fig. 3 shows the E_z profile at $(x = 3\Delta x, y = 3\Delta y)$, from $z = 80\Delta z$ to $z = 120\Delta z$ (the mode is excited at $z = 0$), after 300 time steps. Perfect agreement is shown between the discrete mode propagated with CN–FDTD (dashed line) and its predicted propagation ('+' symbols), while phase differences can be appreciated between the non–discrete mode (sampled in time and in space) propagated with CN–FDTD (continuous line) and its predicted evolution ('◇' symbols) [‖]

[‡] The actual number of discrete modes is limited by the space discretization.

[§] Just for comparison: the non–discrete cut–off frequency is $f_c = 21.20$GHz while the Yee–FDTD discrete one is 21.11 GHz. The FDTD discrete solution is closer to the non–discrete one, as expected, since the dispersion of CN–FDTD is higher than that of the classical Yee FDTD [9].

[‖] This behavior has also been discussed in [28]
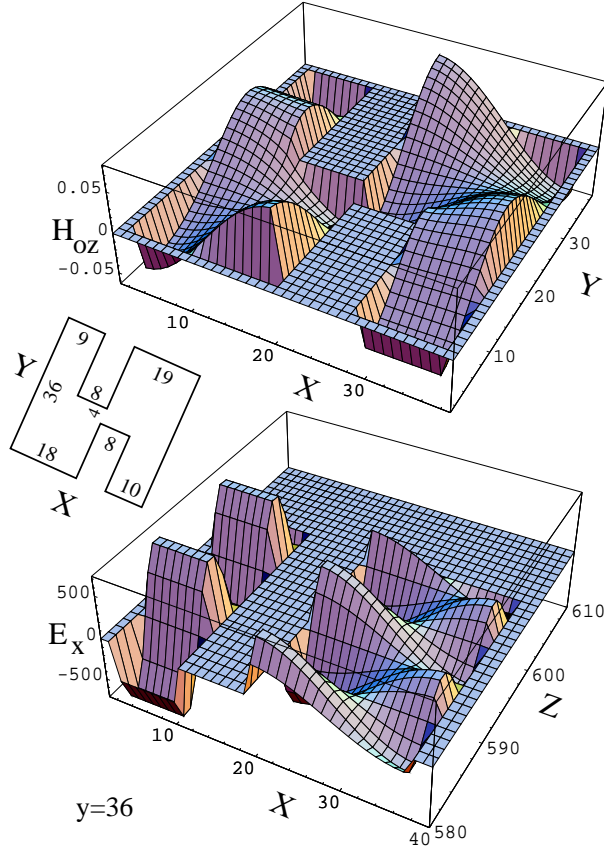
Figure 2. H_{oz} pattern of the 9th TE mode for a ridged rectangular waveguide (top). Geometry of this guide (middle). Propagation along the Z–axis of the E_x component of the 9th mode, at $y = 38$ cells (bottom). All dimensions are in cells ($\Delta x = \Delta y = 333.3$ mm, $\Delta z = 9.0$ mm, $\Delta t = 29.70$ ps)

5. CONCLUSIONS

In this paper we have presented a procedure to obtain the discrete numerical modes propagated by the CN–FDTD method in arbitrarily–shaped metallic waveguides. We have reduced the problem to the solution of an eigenvalue problem, which has been addressed in the general case by numerical techniques, and in an analytical manner for rectangular waveguides.
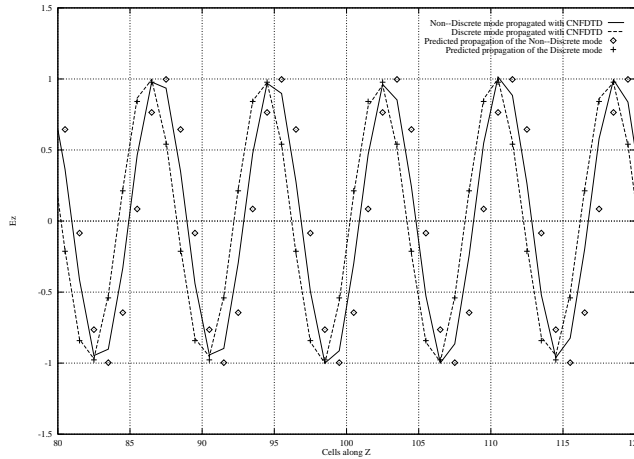
Figure 3. Propagation along the Z–axis of the E_z component of the TM_{11} mode, at $(x = 3\Delta x, y = 3\Delta y)$, in a 6 cell square waveguide. Comparison between different excitations. ($\Delta x = \Delta y = 1.667$ mm, $\Delta z = 1.581$ mm, $\Delta t = 3.12$ ps).

ACKNOWLEDGMENT

REFERENCES

1. K. S. Yee, "Numerical solution of initial boundary value problems involving Maxwell's equations in isotropic media," *IEEE Transactions on Antennas and Propagation*, vol. 14, no. 3, pp. 302–307, Mar. 1966.

2. A. Taflove and S. Hagness, *Computational Electrodynamics: The Finite–Difference Time–Domain Method, 3 ed.* Boston, MA: Artech House, 2005.

3. F. Zheng, Z. Chen, and J. Zhang, "A Finite–Difference Time–Domain method without the Courant stability conditions," *IEEE Microwave Guided Wave Letters*, vol. 9, no. 11, pp. 441–443, 1999.

4. T. Namiki, "A new FDTD algorithm based on Alternating–Direction Implicit method," *IEEE Transactions on Microwave Theory and Techniques*, vol. 47, no. 10, pp. 2003–2007, 1999.

5. E. L. Tan, "Unconditionally stable LOD–FDTD method for 3–D Maxwell's equations," *IEEE Microwave and Wireless Components Letters*, vol. 17, no. 2, pp. 85–87, 2007.

6. F. Liang and G. Wan, "Fourth-order Locally One–Dimensional FDTD method," *Journal of Electromagnetic Waves and Applications*, vol. 22, no. 14–15, pp. 2035–2043, 2008.

7. J. Lee and B. Fornberg, "Some unconditionally stable time stepping methods for the 3D Maxwell's equations," *Journal of Computational and Applied Mathematics*, vol. 166, pp. 497–523, 2004.

8. Salvador G. Garcia, T.-W. Lee, and S. C. Hagness, "On the accuracy of the ADI–FDTD method," *Antennas and Wireless Propagation Letters*, vol. 1, no. 1, pp. 31–34, 2002.

9. S. G. Garcia, R. G. Rubio, A. R. Bretones, and R. G. Martin, "On the dispersion relation of ADI–FDTD," *IEEE Microwave and Wireless Components Letters*, vol. 16, no. 6, pp. 354–356, Jun. 2006.

10. Y. Yang, R. Chen, and E. Yung, "The unconditionally stable Crank–Nicolson FDTD method for three–dimensional Maxwell's equations," *Microwave and Optical Technology Letters*, vol. 48, pp. 1619–1622, 2006.

11. Y. Yang, H. Fan, D. Z. Ding, and S. B. Liu, "Application of the preconditioned GMRES to the Crank–Nicolson Finite-Difference Time–Domain algorithm for 3D full–wave analysis of planar circuits," *Microwave and Optical Technology Letters*, vol. 50, no. 6, pp. 1458–1463, 2008.

12. S. Garcia, R. G. Rubio, A. R. Bretones, and R. G. Lopez,

"Revisiting the stability of Crank–Nicolson and ADI–FDTD," *IEEE Transactions on Antennas and Propagation*, vol. 55, no. 11, pp. 3199–3203, 2007.

13. H. K. Rouf, F. Costen, and S. G. Garcia, "3D Crank–Nicolson Finite Difference Time Domain method for dispersive media," *IET Electronics Letters*, vol. 45, no. 19, pp. 961–962, 2009.

14. H. K. Rouf, F. Costen, S. G. Garcia, and S. Fujino, "On the solution of 3D frequency dependent Crank–Nicolson FDTD scheme," *Journal of Electromagnetic Waves and Applications*, vol. 23, pp. 2163–2175, 2009.

15. H. K. Rouf, F. Costen, and S. G. Garcia, "3D Crank–Nicolson Finite Difference Time Domain method for dispersive media," *IET Electronics Letters*, vol. 45, no. 19, pp. 961–962, 2009.

16. K. Xu, Z. Fan, D. Z. Ding, and R. S. Chen, "GPU accelerated unconditionally stable Crank–Nicolson FDTD method for the analysis of three-dimensional microwave circuits," *Progress in Electromagnetics Research*, vol. 102, pp. 381–395, 2010.

17. M. Celuch-Marcysiak and W. K. Gwarek, "Formal equivalence and efficiency comparison of the FDTD, TLM and SN methods in application to microwave CAD programs," in *21st European Microwave Conference*, vol. 1, 1991, pp. 199–204.

18. C. J. Railton and J. P. McGeehan, "The use of mode templates to improve the accuracy of the Finite Difference Time Domain method," in *21st European Microwave Conference*, vol. 2, 1991, pp. 1278–1283.

19. H. Jin, R. Vahldieck, and S. Xiao, "A full–wave analysis of arbitrary guiding structures using a two dimensional TLM mesh," in *21st European Microwave Conference*, vol. 1, 1991, pp. 205–210.

20. F. Arndt, V. Brankovic, and D. V. Krupezevic, "An improved FDTD full wave analysis for arbitrary guiding structures using a two–dimensional mesh," in *IEEE MTT–S International Microwave Symposium*, vol. 1, 1992, pp. 389–392.

21. A. Asi and L. Shafai, "Dispersion analysis of anisotropic inhomogeneous waveguides using compact 2D–FDTD," *IET Electronics Letters*, vol. 28, no. 15, pp. 1451–1452, 1992.

22. W. K. Gwarek, T. Morawski, and C. Mroczkowski, "Application of the FDTD method to the analysis of circuits described by the two–dimensional vector wave equation," *IEEE Transactions on Microwave Theory and Techniques*, vol. 41, no. 2, pp. 311–317, 1993.

23. S. Xiao, R. Vahldieck, and H. Jin, "Full–wave analysis of guided

wave structures using a novel 2–D FDTD," *Microwave and Guided Wave Letters, IEEE*, vol. 2, no. 5, pp. 165–167, 1992.

24. W. Gwarek and M. Celuch-Marcysiak, "Wide–band S–parameter extraction from FDTD simulations for propagating and evanescent modes in inhomogeneous guides," *IEEE Transactions on Microwave Theory and Techniques*, vol. 51, no. 8, 2003.

25. M. Mrozowski, "Function expansion algorithms for the time–domain analysis of shielded structures supporting electromagnetic waves," *International Journal of Numerical Modelling*, vol. 7, no. 1, pp. 77–84, 1994.

26. M. F. Hadi and S. F. Mahmoud, "Optimizing the compact–FDTD algorithm for electrically large waveguiding structures," *Progress in Electromagnetics Research*, vol. 75, p. 253269, 2007.

27. S. Luo and Z. Chen, "An efficient modal FDTD for absorbing boundary conditions and incident wave generator in waveguide structures," *Progress in Electromagnetics Research*, vol. 68, pp. 229–246, 2007.

28. S. Garcia, A. Bretones, M. Pantoja, and R. Lopez, "Yet another look at FDTD numerical errors," *Antennas and Propagation Magazine, IEEE*, vol. 49, no. 3, pp. 156–161, 2007.